LTH 644

# Progress Towards finding Quark Masses and the QCD scale $\Lambda$ from the Lattice

P.E.L. Rakow[a]

[a] Department of Mathematical Sciences, University of Liverpool, Liverpool L69 3BX, UK

We discuss recent work trying to extract the renormalised quark masses and $\Lambda$, the QCD scale, from dynamical simulations in lattice gauge theory.

## 1. INTRODUCTION

Quark masses and $\Lambda_{QCD}$ are both parameters which are not accessible to direct observation, unlike quantities such as hadron masses which have a very clear meaning both in the continuum and on the lattice. Extraction of either quantity from lattice data inevitably involves both a matching of lattice measurements with continuum measurements and the use of results from perturbation theory.

We can divide the reliance on perturbation theory into two classes. In the most favourable cases all the perturbation theory needed can be performed in the continuum. In this case the technology of perturbation theory is very well-developed, and we can expect to find fairly long perturbative series (often to three loops) for the quantities we need. Less favourable is the case when lattice perturbation theory is needed. The propagators and vertices for lattice perturbation theory are much more complicated, making high order calculations very difficult. However we will see that some impressive progress is being made with lattice perturbation theory too.

The structure of this paper is as follows. First we will discuss renormalisation in general, as this is crucial to producing quark masses defined in a way that can be related to continuum physics. Then we will discuss quark masses, dealing separately with the lighter quarks (up, down and strange) and (in less detail) with the heavier quarks (charm and bottom).

For the light quarks the method we discuss in most detail is the use of the pseudoscalar meson masses to determine the quark masses. From the lowest-order chiral perturbation theory we know that a pseudoscalar meson made of quarks of flavour $a$ and $b$ has its mass given by

$$m_{PS}^2 \propto m_a + m_b \tag{1}$$

which implies that the pseudoscalar meson mass (and especially the $\pi$ mass) will be very sensitive to the quark masses. Eq. (1) also implies that the average light quark mass $m_l \equiv \frac{1}{2}(m_u + m_d)$ will be easier to measure than the separate $u$ and $d$ masses, and in this contribution we will only discuss this averaged light quark mass.

In the second part of the paper we will discuss attempts to fix the scale parameter of QCD, $\Lambda_{QCD}$, both from measurements carried out at "normal" lattice spacings, using gauge configurations generated for other projects, and from fine lattice spacings, using simulations dedicated to the purpose of determining $\Lambda$.

## 2. RENORMALISATION AND $Z$ FACTORS

With very few exceptions, an operator expectation value measured on the lattice has to be renormalised before we can give a number which can be compared with experiment. One can think of this as a calibration factor. Estimating $Z_m$, the renormalisation factor for the quark mass, is one of the more difficult steps in the calculation of quark masses, so it is appropriate to discuss renormalisation in some detail.

There are a handful of cases where the $Z$ factor is not needed (for example, the conserved vector current). In other cases one can do a completely non-perturbative calculation. An example of this is $Z_V$, the renormalisation constant for the local vector current, $\overline{\psi}\gamma_\mu\psi$. We know, from the conservation of baryon number and charge, exactly what the correct answer should be when the matrix element of the vector current is measured in a hadron. This can be used to calculate $Z_V$, e.g. [1]. This calculation does not rely on any perturbation theory at all, neither on the lattice nor in the continuum.

Usually we are not this fortunate, and we have to calibrate our lattice probe by comparing lattice results with continuum perturbation theory results [2]. To use this method one measures quark propagators and Greens functions at a range of virtualities. Because these are gauge-dependent quantities the gauge must be fixed, the usual choice is to impose the Landau gauge. The relation we use to define the renormalisation of an operator $O$ is

$$\Lambda_O^{\overline{MS}} = \frac{Z_O}{Z_\psi}\Lambda_O^{lat}, \tag{2}$$

where $Z_\psi$ is the wave-function renormalisation constant, defined in a similar fashion by comparing the lattice propagator with the $\overline{MS}$ propagator[1].

Where do we get the $\overline{MS}$ Greens functions which we need for this calculation? Here we have to rely on continuum perturbation theory. The results we need to interpret our lattice results are now available up to 3 or 4 loops [3]. Even the continuum perturbation series can be slowly converging in some cases. Tricks to accelerate the series' convergence, such as careful choice of scale, may be helpful.

The comparison between lattice and continuum results must be performed at a scale $\mu$ that satisfies

$$\Lambda_{QCD}^2 \ll \mu^2 \ll 1/a^2. \tag{3}$$

[1]Traditionally the process is split up into two stages by introducing an intermediate renormalisation scheme such as RI or RI′. A renormalisation factor taking us from lattice to RI′ is followed by a conversion factor to change RI′ to $\overline{MS}$. I think the nature of the calculation is easier to follow if we combine both stages, and convert directly from lattice to $\overline{MS}$.

The lower limit arises because when $\mu^2$ is too small we do not know the true value of $\Lambda_O^{\overline{MS}}$, since our perturbative series do not converge fast enough, and because the Greens function may have large non-perturbative contributions, for example contributions associated with the spontaneous breaking of chiral symmetry and the existence of a quark condensate. The upper limit arises because the lattice Greens function will have discretisation errors which become important when $a^2\mu^2 \sim 1$. The method of [2] relies on the existence of a plateau region between these two limits, and in practice this may turn out to be disappointingly narrow.

There is little that can be done about the lower limit, what happens here is a real physical effect, present both on the lattice and in the continuum. On the other hand lattice perturbation theory can be used to greatly reduce the $a^2\mu^2$ errors, extending the useful plateau region outwards.

Normally lattice perturbation theory results are quoted for small external momenta $a^2\mu^2 \ll 1$ but with a little extra effort the Greens functions can be found for any external momentum. Subtracting off the one-loop contribution to the discretisation errors allows us to reduce errors of this type from $O(g^2a^2\mu^2)$ to $O(g^4a^2\mu^2)$. The success of this procedure can be seen in Fig. 1, which shows a much better plateau after subtraction of one-loop lattice artefacts.

### 2.1. Singlet Contribution

We have discussed how to measure the renormalisation constants for quark bilinear operators, but how can we measure the mass renormalisation factor $Z_m$? The usual method is to look for an identity relating $Z_m$ to $Z_S$, the renormalisation factor for the scalar operator.

The usual way to derive this is by looking at the divergence of a flavour non-singlet vector current $J_\mu^a$. In the continuum this current is $\overline{\psi}\gamma_\mu\tau^a\psi$, where $\tau$ is a traceless flavour matrix. The lattice form depends on the fermion action, for Wilson or clover fermions it is

$$\tfrac{1}{2}\overline{\psi}(x+\hat{\mu})[\gamma_\mu + r]\tau^a\psi(x) + \tfrac{1}{2}\overline{\psi}(x)[\gamma_\mu - r]U^\dagger(x)\tau^a\psi(x+\hat{\mu}).$$

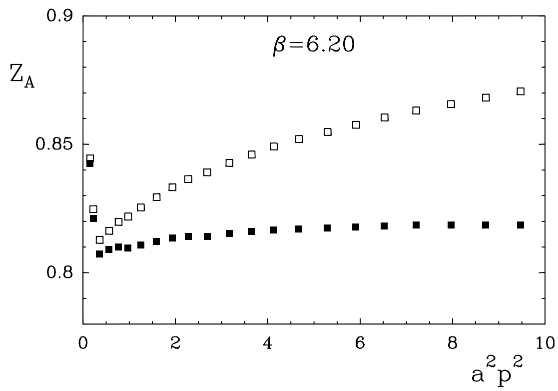


Figure 1. *The renormalisation factor for the axial current, for quenched clover fermions at $\beta = 6.20$. The open squares show the raw data, the black squares show the result after subtraction of the one-loop discretisation errors. The subtraction procedure increases the plateau region.*

The Ward identity [4] reads

$$\langle \partial_\mu J^a_\mu \rangle = \langle \overline{\psi}\ [M, \tau^a]\ \psi \rangle\ + \text{contact terms}, \quad (4)$$

where $M$ is the quark mass matrix. This identity links the flavour non-singlet scalar operator and the flavour non-singlet part of the mass matrix. Eq. (4) is an exact lattice identity if we use the conserved vector current, but because it only involves the non-singlet part of the mass matrix (i.e. mass differences), it still permits an additive renormalisation of the singlet part of the mass matrix (which does of course occur in Wilson or clover fermions).

Requiring that eq. (4) still hold after renormalisation tells us that $Z_m^{NS} Z_{\overline{\psi}\psi}^{NS} = 1$. This tells us how to renormalise non-singlet quantities, such as mass differences, but it doesn't tell us how the singlet part of $M$ (which commutes with $\tau$) renormalises.

In $\overline{MS}$ we are used to having a difference between singlet and non-singlet renormalisation factors for operators with an *odd* number of gamma matrices. Because clover fermions have no exact chiral symmetry, there can be a difference between singlet and non-singlet $Z$ for operators with an *even* number of gamma matrices too. This can be seen in Fig. 2. In the continuum the "bubble" diagram would be the product of 5 gamma matrices (3 from propagators, 2 from $qqg$ vertices) so its trace would be zero in the massless case. For Wilson or clover fermions this no longer holds, and the bubble will give a non-zero contribution.

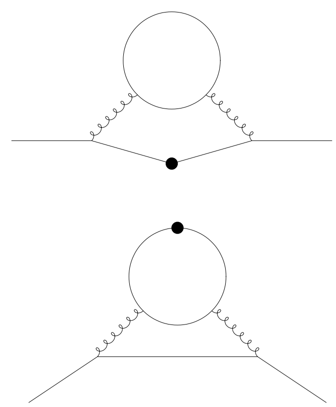

Figure 2. *An example (above) of a Feynman diagram present in both singlet and non-singlet cases, and (below) a diagram which only contributes to the singlet $Z$. The black point shows where the $\overline{\psi}\psi$ operator is inserted.*

The singlet vector current does not give us any useful information about the mass matrix, but we can find some relationships by considering partially quenched QCD, with valence quarks allowed to have a different mass from the sea quark mass. If we change the valence quark mass while keeping the sea quark mass fixed, the derivative of the quark propagator $S$ gives the non-singlet scalar three-point function

$$\frac{\partial}{\partial \frac{1}{2\kappa_{val}}} S(p) = G^{NS}_{\overline{\psi}\psi}(p). \quad (5)$$

However if we change valence and sea quark masses together we get an identity for the singlet scalar three-point function

$$\left( \frac{\partial}{\partial \frac{1}{2\kappa_{val}}} + \frac{\partial}{\partial \frac{1}{2\kappa_{sea}}} \right) S(p) = G^{S}_{\overline{\psi}\psi}(p)\ . \quad (6)$$

From these identities we conclude that $Z_m^{NS} Z_{\overline{\psi}\psi}^{NS} = 1$ (which we already knew from the

Vector Ward Identity) and $Z_m^S Z_{\overline{\psi}\psi}^S = 1$ which is new. We can find $Z_{\overline{\psi}\psi}^{NS}$ and thus $Z_m^{NS}$ by the non-perturbative methods discussed earlier. The identities here also give us a way of finding $Z_m^S$.

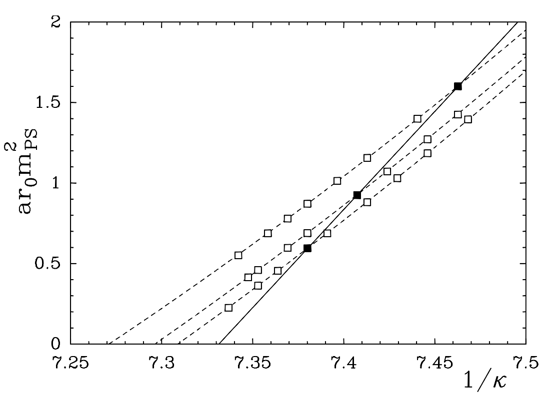


Figure 3. *Dynamical and partially quenched pseudoscalar meson masses for clover fermions at $\beta = 5.29$. Data from [5].*

In Fig. 3 we show partially quenched (open points) and full dynamical (filled points) data for the pseudoscalar meson masses. We can immediately see that there is a different critical $\kappa$ if we follow the solid line connecting the full dynamical points (the points with valence and sea quark masses equal) than if we follow one of the dashed lines (sea quark mass held fixed, valence quark mass varied). This is because clover fermions have no exact chiral symmetry, and so an additive quark mass renormalisation is possible. The difference in critical $\kappa$s shows that this additive term depends quite strongly on the sea quark mass.

In the continuum the situation would look quite different — because of chiral symmetry both the full and partially quenched curves would both have to pass through the origin, at zero valence quark mass. This would also apply for a lattice fermion formulation (such as overlap fermions) which have an exact chiral symmetry. After renormalisation the lattice results ought to show the same structure, with both full dynamical and partially quenched $m_{PS}$ vanishing at the same place. The only way to arrange this is to use different renormalisation factors for the partially quenched and full QCD quark masses, see Fig. 4, just as we expected from considering the identities eqs. (5) and (6).

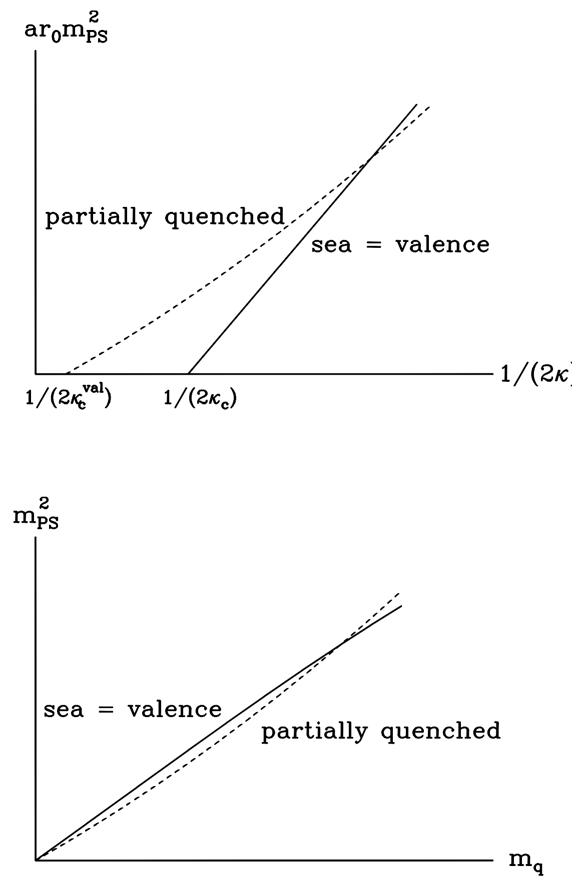


Figure 4. *Dynamical and partially quenched pseudoscalar meson masses before and after renormalisation of the quark mass.*

We define the bare sea and valence quark masses by

$$m = \frac{1}{2\kappa} - \frac{1}{2\kappa_c}, \tag{7}$$

with $\kappa_c$ defined as the critical $\kappa$ for QCD with equal valence and sea quark masses (see Fig. 4). The renormalised masses are then defined by

$$\begin{aligned} m_{sea}^R &= Z_m^S m_{sea} \ , \\ m_{val}^R &= Z_m^{NS}(m_{val} - m_{sea}) + Z_m^S m_{sea} . \end{aligned} \tag{8}$$

The partially quenched pseudoscalar mesons are massless at the point where $m_{val}^R = 0$, which we call $\kappa_c^{val}$. We can use this to find the ratio of the two $Z$'s,

$$\frac{Z_m^S}{Z_m^{NS}} = \left. \frac{m_{sea} - m_{val}}{m_{sea}} \right|_{\kappa_{val} = \kappa_{val}^c} \tag{9}$$

$$= \left( \frac{1}{2\kappa_{sea}} - \frac{1}{2\kappa_{val}^c} \right) \left( \frac{1}{2\kappa_{sea}} - \frac{1}{2\kappa^c} \right)^{-1} .$$

$Z$ ratios calculated this way in [5] are shown in Fig. 5. The ratio only depends weakly on the quark mass, but it depends very strongly on $\beta$. The ratio drops rapidly as lattice spacing decreases.

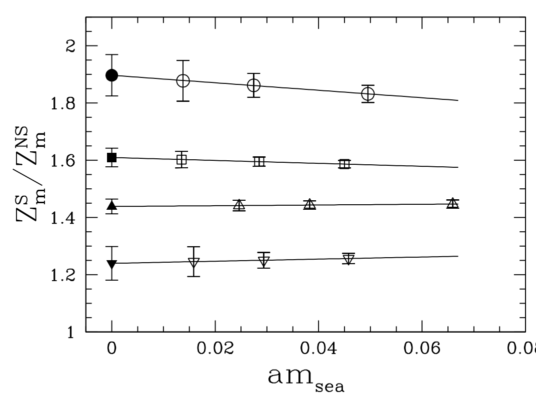


Figure 5. *The ratio $Z_m^S/Z_m^{NS}$ for dynamical clover fermions [5]. $\beta$ values run from 5.20 (highest line) to 5.40 (lowest line).*

One way to illustrate the importance of the ratio $Z_m^S/Z_m^{NS}$ is to go back to one of the pioneering dynamical calculations [6], carried out with two flavours of unimproved Wilson fermions. In this paper they initially found a value for the ratio $m_s/m_l \approx 52$, which is a long way from the value found in quenched calculations, and also far from the predictions of chiral perturbation theory

$$\frac{m_s}{m_l} = \frac{2m_K^2 - m_\pi^2}{m_\pi^2} \approx 25 \ . \tag{10}$$

Normally one would expect the mass renormalisation factor to cancel out in this ratio, but because the singlet and non-singlet $Z$ differ this is not entirely true.

In Fig. 6 we show a pion line, the line giving the pseudoscalar mass when valence and sea quark masses are equal, and the kaon line, showing the result when sea quarks and one valence quark (representing the $u$ or $d$ in the $K$) are kept at a fixed mass, while the other valence quark (representing the strange quark) is varied. The slopes of these two lines are different, just as seen in the partially quenched case.

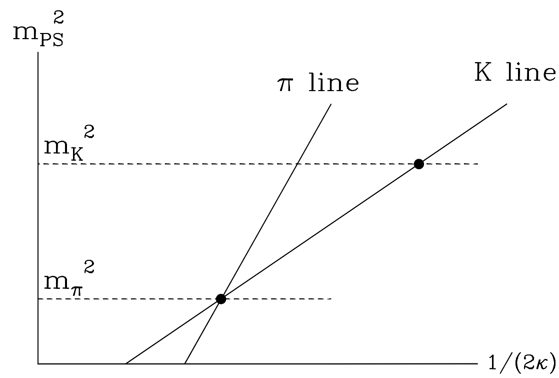


Figure 6. *A schematic diagram illustrating the subtleties of measuring the strange/light quark mass ratio from Wilson fermions.*

We determine the $\kappa$ corresponding to the light quark mass by seeing where the $\pi$ line crosses the mass-squared of the real physical pion, and the strange quark $\kappa$ by seeing where the kaon line crosses the mass-squared of the physical $K$. If we now use these two $\kappa$ values to calculate the ratio of the *bare* quark masses, $m_s^{bare}/m_l^{bare}$ we get a ratio much larger than from eq. (10), because the $K$ line in Fig. 6 is less steep than the $\pi$ line. However, if we renormalise the masses according to eq. (8), then the slopes of the kaon and pion lines will become approximately equal, as in the lower panel of Fig. 4, and now the ratio of the *renormalised* quark masses will be close to eq. (10).

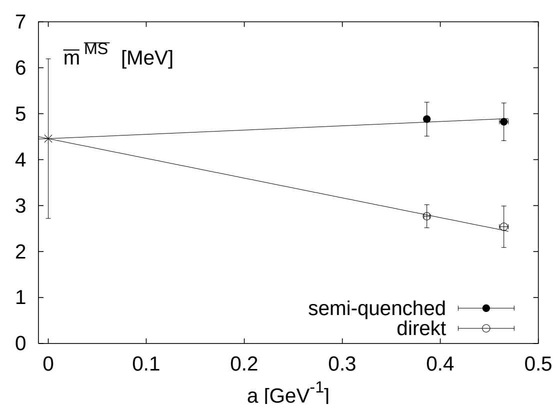


Figure 7. *A figure from [7] showing the difference in light quark masses found from partially quenched and fully dynamical ("direkt") data.*

In later works [7] the SESAM collaboration used a different strategy, measuring data from both partially quenched and fully dynamical mesons, and then making a joint extrapolation to the continuum limit, Fig. 7. The same $Z$ was used in both cases. This gives a result more in line with what we do here, but it is not exactly the same. Although we have seen in Fig. 5 that the ratio $Z_m^S/Z_m^{NS}$ decreases as $a$ decreases, there will presumably be a perturbative contribution at the two-loop level, which means that the $Z$ ratio will asymptotically approach the value 1 rather slowly, like $1+O(g^4)$, rather than like a power of $a$, so one will not be able to completely remove this effect by power-law extrapolations in $a$.

The argument we give here, using different $Z$ factors for the singlet and non-singlet parts of the mass matrix is rather similar to the discussion given at Lattice '97 in [8].

### 2.2. Quark mass results

The preliminaries are now over, and it is time to discuss some of the recent quark mass results from dynamical simulations.

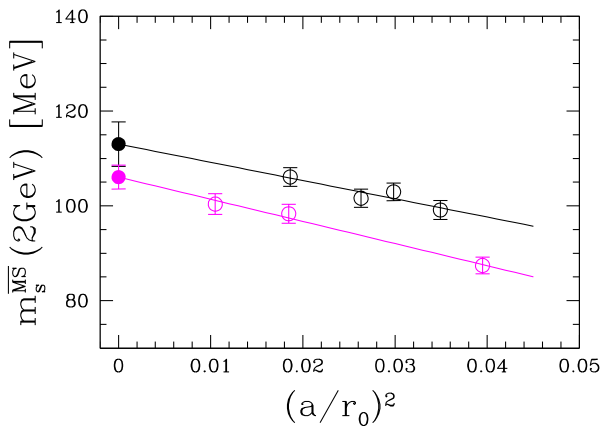


Figure 8. *A comparison of quenched (above) and dynamical (below) estimates for the strange quark mass [5].*

In Fig. 8 we show an estimate of the strange quark mass calculated using the flavour-singlet renormalisation constant calculated from the comparison of dynamical and partially quenched mesons. The result is rather similar to that found in the quenched case. If the non-singlet renormalisation constant had been used the $a$-dependence would be much stronger, and the data points would have been lower.

An alternative mass definition is based on the continuum Ward identity for an axial current with flavour index $a$ [4],

$$\langle \partial_\mu A_\mu^a \rangle = \langle \overline{\psi} \{m, \tau^a\} \gamma_5 \psi \rangle + \text{contact terms.} \quad (11)$$

In clover fermions the axial current has to be improved by adding irrelevant operators, because of the lack of a true chiral symmetry. As can be seen from the Ward identity, this axial Ward identity (AWI) mass has to be renormalised by the factor

$$m^{ren} = \frac{Z_A}{Z_P} m^{AWI} \ . \quad (12)$$

The final renormalised result ought to be the same in either case, but we will see that this is not yet the case, there are still fairly large differences between different groups working on this problem.

The AWI quark mass definition has been used by the CP-PACS and JLQCD Collaborations to study the quark masses in clover QCD, both for two-flavour [9] and (2+1) flavour simulations [10]. The $Z$ ratio needed to renormalise the bare lattice masses are calculated from tadpole-improved one-loop lattice perturbation theory. Their results are summarised in Fig. 9. In the quenched case the result depends quite heavily on whether the $K$ or $\phi$ meson is used to determine the strange quark mass. This is a sign that the quenched theory differs from the real world. Fortunately this discrepancy is greatly reduced when sea quarks are switched on, as can be seen in the panels of Fig. 9 showing the $s$ quark mass from dynamical QCD.

The SPQcdR Collaboration [11] have measured quark masses in an $N_f = 2$ simulation using the Wilson quark action at a single $\beta$ value, $\beta = 5.8$. They use both the VWI and AWI definitions of quark mass, and find compatible results from both methods. The renormalisation constants are found non-perturbatively using the method of [2]. Their preliminary values are included in Table 1, and are broadly compatible with the results of [5].

In [12] the quark masses are measured in a dynamical simulation with (2+1) flavours of sea quark. The use of staggered quarks speeds up the calculation considerably, allowing the light $u/d$ sea quarks to be simulated all the way down to

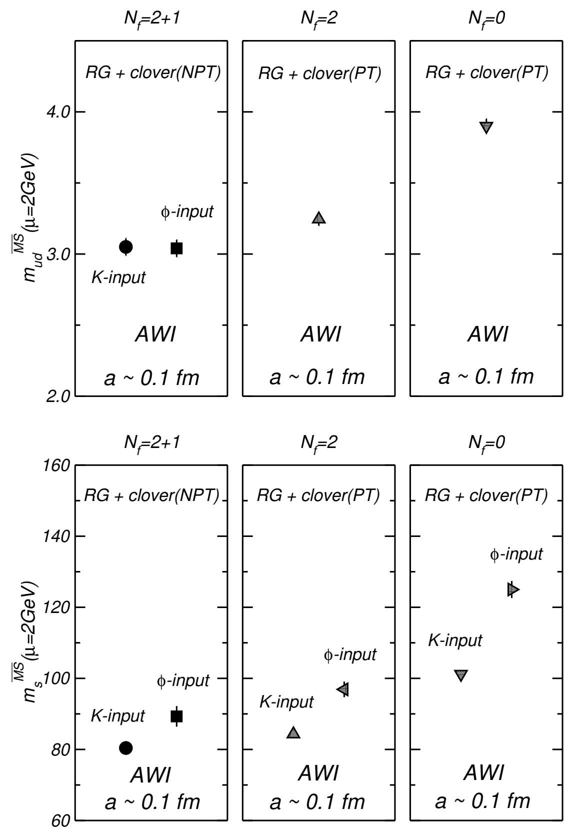


Figure 9. *The $u$ and $d$ quark masses (above) and $s$ quark mass (below) at $a \sim 0.1$ fm, from [10].*

masses $\sim m_s/8$, a considerable advance on what is possible with other quark formulations. The staggered quarks have been improved to suppress 'taste' violation and other discretisation errors. This also has the effect of making perturbation theory better behaved than it is for unimproved staggered fermions. The $Z$ factors used in [12] are calculated in one-loop tadpole improved perturbation theory. The estimated error due to the unknown higher-order terms in perturbation theory is 9%. This study finds that the effects of including sea quarks are dramatic, and that the final physical masses of the quarks are a lot lighter in the dynamical simulation than they were in a quenched calculation.

Fig. 10 shows determinations of the strange quark mass compiled by the Particle Data

| $m_l$/MeV | $m_s$/MeV | sea quarks | Reference |
|---|---|---|---|
| 3.05(6) | 80.4(1.9) | (2+1) | CP-PACS and JLQCD [10] |
| 2.8(0)(1)(3)(0) | 76(0)(3)(7)(0) | (2+1) | HPQCD, MILC and UKQCD [12] |
| 4.7(2)(3) | 119(5)(8) | $N_f = 2$ | QCDSF/UKQCD [5] |
| 4.8(5) | 111(6) | $N_f = 2$ | SPQcdR Collaboration [11] |
| 4.5(17) | | $N_f = 2$ | SESAM/T$\chi$L [7] |

Table 1
*Masses of the light, $m_l = \frac{1}{2}(m_u + m_d)$, and strange quarks in dynamical lattice QCD, as determined by various collaborations. The masses are given in the $\overline{MS}$ scheme at a scale of 2 GeV.*

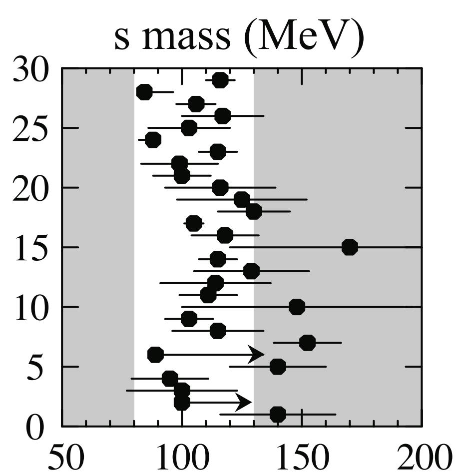


Figure 10. *Determinations of the strange quark mass from the Particle Data Group [13].*

Group [13]. Comparing this with Table 1 we see that most of the dynamical lattice determinations look low compared with estimates from traditional methods.

### 2.3. The charm quark mass

The charm quark mass has its own special difficulties because $m_c$ is comparable with the inverse lattice spacing $a^{-1}$ for the lattice spacings we have to work with at present. This means that lattice artefacts proportional to high powers of $am_c$ can be important, so it would be useful to have expressions resumming all $(am_c)^n$ terms. Suggestions on how to do this (known as FNAL masses) were made in [14]. As the lattice spacing becomes smaller all definitions should agree. This is examined in [15], where the charm mass determined from the axial and vector Ward identity definitions, and the mass determined from the FNAL method $m_1$ and $m_2$ are compared in the quenched case (where the $a$ range can be made large). At present lattice spacings the mass from the Axial Ward Identity ($m_A$) looks as if it might extrapolate to a lower value than the others, though there is still room for it to move up again, see Fig. 11.

This reference also looks at the effect of finding $m_c$ on dynamical clover configurations, the open symbols on the right-hand side of Fig. 11. There seems to be very little difference between the quenched and dynamical results, though of course the present results are at a single rather coarse lattice spacing, and the sea quarks in the simulation are rather heavy.

### 2.4. $b$ quark mass

A nice example of the interplay between perturbation theory and physical result is the $b$ quark mass calculation of Gimenez, Giusti, Rapuano and Martinelli [16] converting lattice data into a value for $m_b$ in $\overline{MS}$, using stochastic perturbation theory results from [17].

This requires perturbation theory in two places, the conversion from the lattice mass parameter of heavy quark effective theory (HQET) to the pole mass requires the subtraction of a residual mass $\delta m$ which is proportional to $1/a$. This subtraction can be calculated in lattice perturbation theory.

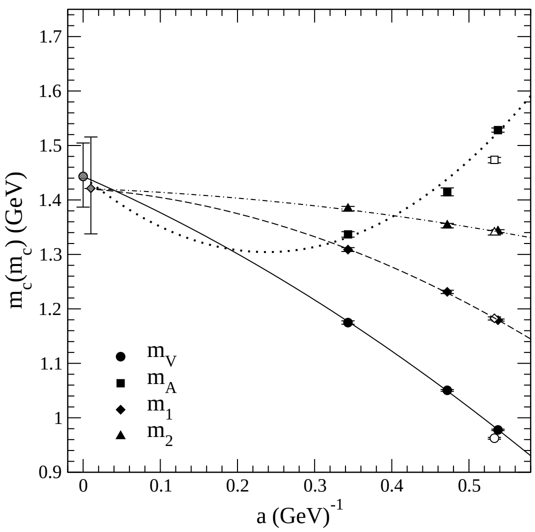


Figure 11. *Different determinations of the charm quark mass [15]. The closed symbols show the effect of using different mass definitions in the quenched case. All definitions should lead to the same continuum value. The open symbols at the right show the charmed quark mass determined on $N_f = 2$ dynamical configurations from UKQCD.*

After that, the conversion from pole mass to $\overline{MS}$ mass is done using results from continuum perturbation theory. Since the $b$ quark pole mass is just used as an intermediate step the calculation taken as a whole is presumably legitimate even though confinement means that there is no pole in the $b$-quark propagator.

The two-loop subtraction for the residual mass was calculated using traditional lattice perturbation theory methods in [18]. The three-loop result was calculated using the novel method of stochastic perturbation theory, which has the major advantage that the difficulty of calculating new terms in the series does not increase as rapidly as it does in conventional calculations. Stochastic perturbation theory thus promises to overtake conventional techniques in the future. It does have some disadvantages, being a stochastic method, the coefficients calculated do have a statistical error, and can not be given to the number of decimal places that we are used to from conventional perturbation theory, but they are usually quite good enough for comparison with real lattice data.

The dependence of the final $b$ quark mass on the order of lattice perturbation theory used is illustrated in Table 2. Knowing the three-loop coefficient helps to significantly reduce the systematic uncertainty in the final estimate, which is

$$\overline{m}_b(\overline{m}_b)|_{unq} = (4.21 \pm 0.03 \pm 0.05 \pm 0.04)\ \mathrm{GeV}.$$

## 3. DETERMINING $\Lambda$

An important (but difficult) project for the lattice is to link the low-energy, non-perturbative quantities we normally measure (such as hadron masses) with the high-energy world accessible in accelerators, where perturbative QCD works well. The key to bridging this gap is to find a value for $\Lambda$, the scale parameter of QCD.

The strategy for determining $\Lambda$ has two necessary parts. Firstly some dimensionful quantity has to be measured to set the scale. A common choice is to look at the static potential. This can be measured fairly well. A good way to fix a length scale is to find the distance at which

$$r^2 F(r) \equiv -r^2 \frac{d}{dr} V(r) \qquad (13)$$

has a particular value [19], the usual value chosen is 1.65, which gives a distance scale $r_0 \approx 0.5 fm$. Another way to find a length scale from the potential, now less popular, would be to use the string tension.

Secondly, we need to extract the $\overline{MS}$ coupling at a known scale, which can then be converted into a value for $\Lambda_{\overline{MS}}$. One possibility is to use lattice perturbation theory to relate the lattice coupling $g^2 = 6/\beta$ to $g^2_{\overline{MS}}$.

Relating the $\Lambda$ parameters of two schemes is a finite calculation. This is an asymptotic statement, and can be answered completely by a one-loop calculation [20].

However, relating the coupling constants at a finite scale is no longer so simple. Outside the

| $\overline{m}_b(\overline{m}_b)$ | Dependence on higher orders (unquenched data) | | | | |
|---|---|---|---|---|---|
| Order | $\delta m$ | $m_b^{pole}$ | $\overline{m}_b(\overline{m}_b)/m_b^{pole}$ | $\overline{m}_b(\overline{m}_b)$ | $\Delta m_b$ |
| LO | 0 | 3770 | 1.000 | 3770 | – |
| NLO | 978.79 | 4748.79 | 0.92276 | 4382 | 612 |
| NNLO | 10.53 | 4759.32 | 0.89060 | 4239 | 143 |
| NNNLO | 74.55 | 4833.87 | 0.86883 | 4200 | 39 |

Table 2
*A table illustrating the way in which the estimate for the bottom quark mass $m_b(m_b)$ depends on the order of the lattice perturbation theory used. The quark mass results are preliminary values from [16], using perturbative calculations from [17] and [18].*

asymptotic regime we need calculations of the $\beta$-function of both schemes to as high an order as possible, this can then be translated into a relation between the couplings. Currently we know the lattice $\beta$ function to three loops [21].

As often happens with lattice perturbation theory we find that the series converge rather poorly. Fortunately we have several methods to accelerate the convergence. One explanation for the large coefficients in lattice perturbation theory is that they come from gluon "tadpoles" due to the higher order vertices present on the lattice [22]. A way to take these into account is to re-express the series in terms of a "boosted" coupling, $g^2_\Box = g^2/U^{plaq}$:

$$\begin{aligned}
\frac{1}{g^2_{\overline{MS}}(\frac{1}{a})} &= \frac{1}{g^2} - 0.4682013 - 0.0556675 g^2, \\
\frac{1}{g^2_{\overline{MS}}(\frac{1}{a})} &= \frac{1}{g^2_\Box} - 0.1348680 - 0.0217565 g^2_\Box, \\
\frac{1}{g^2_{\overline{MS}}(\frac{2.63}{a})} &= \frac{1}{g^2_\Box} \qquad\qquad - 0.013837 g^2_\Box. \qquad (14)
\end{aligned}$$

Using the quenched case as an example we can see in the equation above that the coefficients in the series for the $\overline{MS}$ coupling are reduced when we change the expansion parameter from $g^2$ to $g^2_\Box$. We can improve the series further by choosing a natural scale [23]. If, instead of $g^2_{\overline{MS}}(1/a)$ we calculate $g^2_{\overline{MS}}(2.63/a)$, the $g^0_\Box$ term vanishes, and the first correction is $O(g^2_\Box)$ with a rather small coefficient. This gives us grounds to hope that the unknown higher-order coefficients will not seriously change the estimate of $g^2_{\overline{MS}}$.

Once we have values for $g^2_{\overline{MS}}$ we can use the known $\beta$ function to convert these into a value for $\Lambda^{\overline{MS}}$. The results in the quenched case [24], based on data from [25] and [26], are shown in Fig. 12.

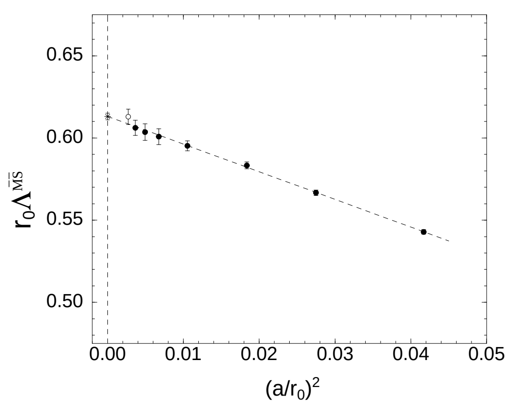


Figure 12. *$\Lambda^{\overline{MS}}$ calculated for quenched QCD for $\beta$ values in the range 5.95 to 6.92 [24]. The $r_0$ values for high $\beta$ are from [26]. The data extrapolates very smoothly towards a value $\Lambda^{\overline{MS}}_{N_f=0} = 242(11)(10) MeV$.*

Some extrapolation in $a$ is needed, this seems not to present any great problem, the data look surprisingly linear in $a^2$, and the smallest $a$ values are close to the continuum limit. The result in physical units is $\Lambda^{\overline{MS}}_{N_f=0} = 242(11)(10) MeV$. The first error is a statistical error, the second error is an attempt to estimate the possible effects of the unknown higher order terms in the $\beta$ functions.

One can try a similar calculation for the dynamical case, using the clover action configurations produced by the UKQCD/QCDSF Collaborations. The lattice $\beta$ function for clover quarks is available [21]. In the dynamical case we need a double extrapolation, both in lattice spacing and in sea quark mass. Both these extrapolations are over a rather large distance. A simple phenomenological extrapolation formula is

$$r_0\Lambda^{\overline{MS}} = const + B(a/r_0)^2 + Cam_q + Dr_0m_q \ . \quad (15)$$

The formula fits the data fairly well, as can be seen in Fig. 13.

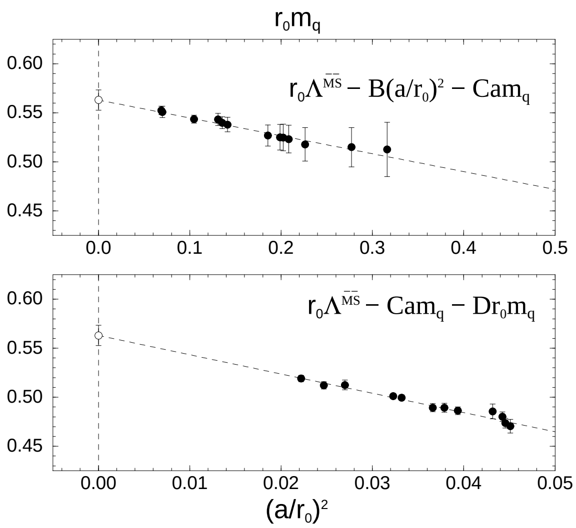


Figure 13. *Extrapolation of $\Lambda^{\overline{MS}}$ for dynamical quarks. The data are measured on UKQCD/QCDSF configurations with dynamical clover fermions [24]. The upper part of the figure shows the mass dependence after the data has been extrapolated to the continuum limit. The lower half shows the a dependence of data after extrapolating to the chiral limit.*

The extrapolated value hasn't changed very much due to the jump to finer lattice spacings in the past year [24], the new value is $\Lambda = 222(4)(28) MeV$ at $N_f = 2$.

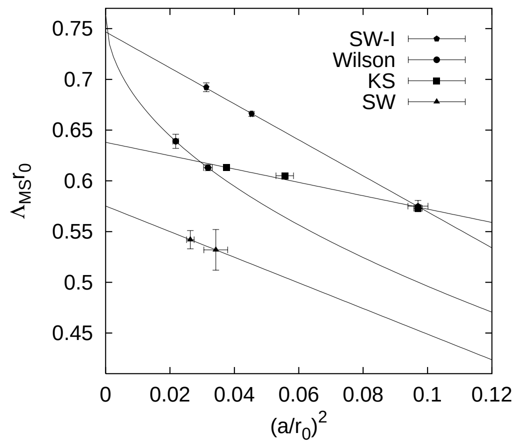


Figure 14. *A comparison of continuum extrapolations of $r_0\Lambda^{\overline{MS}}$ [27] made for various fermion actions. Wilson fermions are extrapolated linearly in a, while clover and staggered are extrapolated linearly in $a^2$.*

One way to estimate the systematic error in the final result is to repeat the calculation for different formulations of dynamical fermions, and see how much the results scatter. A very complete study was carried out in [27]. As can be seen in Fig. 14 the results do still depend quite a lot on the action and extrapolation procedure. The dependence on the action could be due in part to higher order terms in the perturbation series, which will of course depend on the fermions used.

A very impressive attack on finding $\Lambda$ was reported in this year's Lattice Conference [28], extending work done in [29] with Asqtad improved staggered fermions. Extensive three-loop calculations of Wilson loops and the static potential have been carried out. Some idea of the work involved can be gained by looking at the number of Feynman diagrams that have to be considered, Fig. 15. Wilson loops of different sizes are dominated by gluons of different virtualities, with small loops corresponding to large $Q^2$. Thus by calculating $\alpha_s$ from loops of different sizes one can see how $\alpha_s$ runs even from data taken at a single value of $a$. This is illustrated in Fig. 16, where one can see how well the running of $\alpha$ agrees with the $\beta$ function predictions.

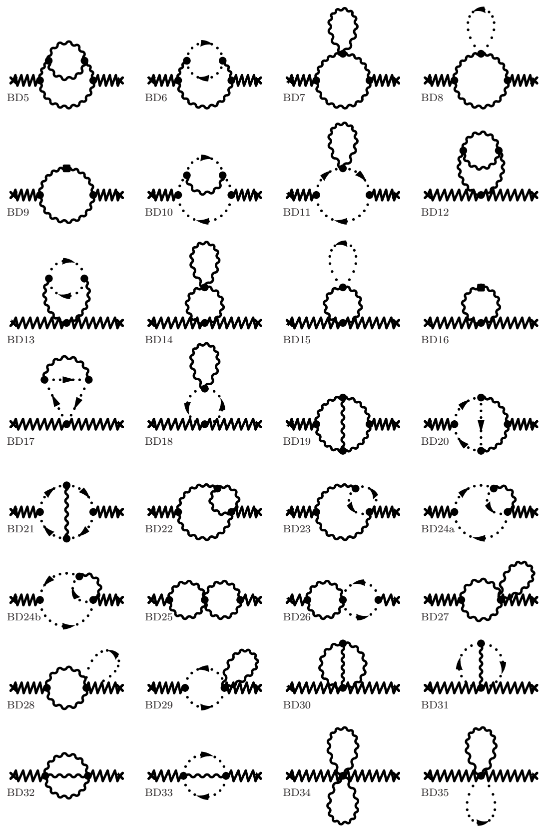


Figure 15. *The gluon and ghost Feynman diagrams used in [28] to calculate three-loop results for Wilson loops and the static potential. A similar number of fermion loop diagrams is needed to calculate the unquenched case.*

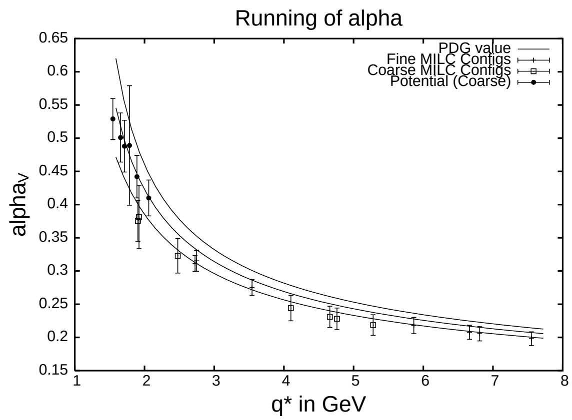


Figure 16. *The running of $\alpha_s$ as determined by [28]. $\alpha_s$ is defined in the potential scheme.*

In Fig. 17 we see the lattice results extrapolated out to the scale $m_Z$, where they are compared with the traditional Particle Data Group value. The agreement looks impressively good.

Is there any way of diminishing the dependence on high-order perturbation theory? The obvious way to reduce our sensitivity to high order terms in the perturbation theory is to work at weaker values of the coupling — in QCD this means working at high energy or short distance. This requires a very fine lattice spacing, $a$, which in turn forces us to consider simulations in small physical volumes. The small volumes involved in this method mean that it isn't possible to reuse configurations generated for other projects on hadronic physics, the calculations require many dedicated runs at very large $\beta$ values.

The ALPHA Collaboration have been pursuing this method for many years [30], using the same methods that they applied in the quenched case [31]. A recent plot of their results is shown in Fig. 18. By repeatedly halving the lattice spacing (and the physical size $L$ of their system), they make measurements of $\alpha_s$ over a large range of scales (more than two orders-of-magnitude). These are compared with the running expected from the three-loop $\beta$ function. The data reach $\alpha_s$ values $\sim 0.1$, where we are very confident that perturbation theory will work well. As can be seen, the agreement with the perturbative $\beta$ function remains close, except perhaps at the very lowest scale. The fact that perturbation theory works so well over such a large range offers some comfort to the groups that base their determination of $\Lambda$ on lattices with "normal" lattice spacings, who have to rely on data with $\mu/\Lambda$ around

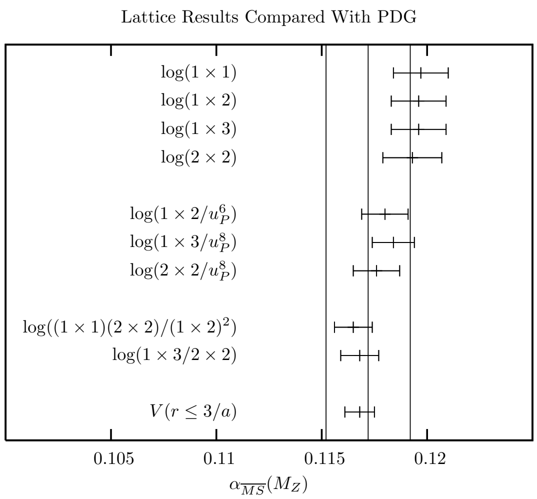


Figure 17. $\alpha_s(m_Z)$ *estimated from Wilson loops of various sizes, and from the short distance potential [28].*

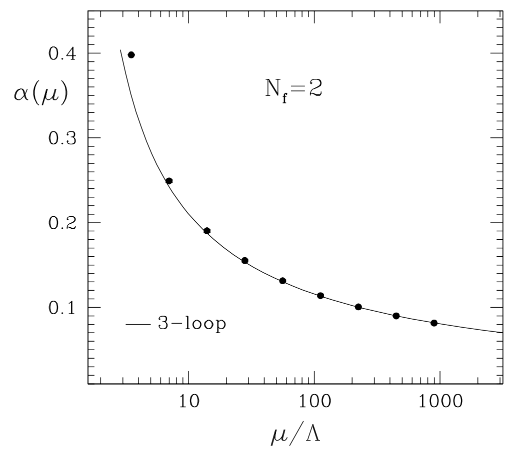


Figure 18. *The running of* $\alpha_s$ *in two-flavour dynamical QCD as determined by the ALPHA Collaboration [30].*

10 or 20, but clearly the precision that will be achieved from data at $\mu/\Lambda \sim 1000$ should be much greater.

This work has not yet given a final value for $\Lambda$ in physical units, preliminary results give the value $\ln(\Lambda L_{max}) = -1.34(7)$ where $\alpha_s(L_{max}) = 0.372$, but the final step is still needed, a conversion from the length scale they use, $L_{max}$, to physical units.

## 4. CONCLUSIONS

The determination of quark masses is the more mature of the two fields we have looked at. We see that agreement has not yet been reached, and there are still differences between the measurements of the different groups. It is not yet clear (to me at least) where the origin of these differences lies, as there are many differences between the calculations, particularly in the ways the $Z$ factors are calculated and in the choice of mass definition.

One area in which we are making progress, and can expect more advances in the coming years, is bringing the sea quark masses down towards more realistic values. When simulations are carried out with large sea quark masses it can be difficult to find much difference from quenched calculations, and the extrapolation to the physical region can be difficult. Now, with more powerful machines and new fermion actions, we are seeing simulations carried out much closer to the physical region, and we can expect more soon.

A topic which we have not covered here is the calculation of quark masses using overlap fermions, since dynamical overlap is not yet as advanced as dynamical calculations with the older fermion formulations.

In both the calculation of masses and of $\Lambda$ we have a need for higher orders of perturbation theory. Advances in lattice simulations are making lattice perturbation theory more difficult, because more complicated actions lead to more complicated Feynman rules, and because there is now far greater diversity in the choice of fermion and gauge actions used. At Lattice '04 we have seen that diagrammatic techniques are rising to the challenge, we have also seen that stochastic perturbation theory is delivering results which are useful to those extracting physics from lattice simulations.

## REFERENCES


1. T. Bakeyev, M. Göckeler, R. Horsley, D. Pleiter, P.E.L. Rakow, G. Schierholz and H. Stüben (QCDSF-UKQCD Collaboration), Phys. Lett. B **580** (2004) 197.
2. G. Martinelli, C. Pittori, C.T. Sachrajda, M. Testa and A. Vladikas, Nucl. Phys. B **445** (1995) 81.
3. K.G. Chetyrkin and A. Retey, Nucl. Phys. B **583** (2000) 3; J.A. Gracey, Nucl. Phys. B **662** (2003) 247; Nucl. Phys. B **667** (2003) 242.
4. I. Montvay and G. Münster, "Quantum Fields on a Lattice", Cambridge University Press (1994).
5. M. Göckeler, R. Horsley, A.C. Irving, D. Pleiter, P.E.L. Rakow, G. Schierholz and H. Stüben, arXiv:hep-ph/0409312.
6. N. Eicker *et al.* [SESAM Collaboration], Phys. Lett. B **407** (1997) 290.
7. N. Eicker *et al.* (SESAM/T$\chi$L Collaboration) Nucl. Phys. Proc. Suppl. **106** (2002) 209.
8. T. Bhattacharya and R. Gupta, Nucl. Phys. Proc. Suppl. **63** (1998) 95.
9. A. Ali Khan *et al.* [CP-PACS Collaboration], Phys. Rev. D **65** (2002) 054505. [Erratum-ibid. D **67** (2003) 059901].
10. T. Ishikawa *et al.*, (CP-PACS and JLQCD Collaborations) [arXiv:hep-lat/0409124].
11. D. Becirevic *et al.*, (SPQcdR Collaboration), arXiv:hep-lat/0409110.
12. C. Aubin *et al.* (HPQCD, MILC and UKQCD Collaborations) Phys. Rev. D70 (2004) 031504; C. Aubin *et al.* (MILC Collaboration), arXiv:hep-lat/0407028.
13. S. Eidelman *et al.*, Phys. Lett. **B592**, 1 (2004).
14. B.P.G. Mertens, A.S. Kronfeld and A.X. El-Khadra, Phys. Rev. **D58** (1998) 034505.
15. A. Dougal, C.M. Maynard and C. McNeile, arXiv:hep-lat/0409089.
16. V. Gimenez, personal communication.
17. F. Di Renzo and L. Scorzato, arXiv:hep-lat/0410010.
18. G. Martinelli and C.T. Sachrajda, Nucl. Phys. **B 559** (1999) 429.
19. R. Sommer, Nucl. Phys. B **411** (1994) 839.
20. A. Hasenfratz and P. Hasenfratz, Phys. Lett. B **93** (1980) 165; A. Hasenfratz and P. Hasenfratz, Nucl. Phys. B **193** (1981) 210; P. Weisz, Phys. Lett. B **100** (1981) 331; R. Dashen and D.J. Gross, Phys. Rev. D **23** (1981) 2340.
21. C. Christou, A. Feo, H. Panagopoulos and E. Vicari, Nucl. Phys. B **525** (1998) 387 [Erratum-ibid. B **608** (2001) 479]; A. Bode and H. Panagopoulos, Nucl. Phys. B **625** (2002) 198.
22. G.P. Lepage and P.B. Mackenzie, Phys. Rev. D **48**, 2250 (1993).
23. M. Lüscher, arXiv:hep-lat/9802029.
24. M. Göckeler, R. Horsley, A.C. Irving, D. Pleiter, P.E.L. Rakow, G. Schierholz, H. Stüben, (QCDSF-UKQCD Collaboration), arXiv:hep-lat/0409166.
25. S. Booth *et al.* (QCDSF-UKQCD Collaboration), Phys. Lett. B **519** (2001) 229.
26. S. Necco and R. Sommer, Nucl. Phys. B **622** (2002) 328.
27. G. Bali and P. Boyle, arXiv:hep-lat/0210033.
28. Q. Mason, these proceedings.
29. C. Davies *et al.*, (HPQCD and UKQCD Collaborations) Nucl. Phys. Proc. Suppl. **119** (2003) 595
30. A. Bode *et al.*, Phys. Lett. B 515 (2001) 49; M. Della Morte *et al.*, Nucl. Phys. Proc. Suppl. **119** (2003) 439.
31. S. Capitani, M. Lüscher, R. Sommer and H. Wittig (ALPHA Collaboration), Nucl. Phys. B **544** (1999) 669.